ITER Test Blanket Module Error Field Simulation Experiments at DIII-D

M.J. Schaffer 1), J.A. Snipes 2), P. Gohil 1), P. de Vries 3), T.E. Evans 1),
M.E. Fenstermacher 4), X. Gao 5), A.M. Garofalo 1), D.A. Gates 6), C.M. Greenfield 1),
W.W. Heidbrink 7), G.J. Kramer 6), R.J. La Haye 1), S. Liu 5), A. Loarte 2),
M.F.F. Nave 8), T.H. Osborne 1), N. Oyama 9), J-K. Park 6), N. Ramasubramanian 10),
H. Reimerdes 11), G. Saibene 12), A. Salmi 13), K. Shinohara 9), D.A. Spong 14),
W.M. Solomon 6), T. Tala 15), J.A. Boedo 16), V. Chuyanov 2), E.J. Doyle 17),
M. Jakubowski 18), H. Jhang 19), R.M. Nazikian 6), V.D. Pustovitov 20), O. Schmitz 21),
R. Srinivasan 10), T.S. Taylor 1), M.R. Wade 1), K-I. You 19) L. Zeng 17),
and the DIII-D Team

1) General Atomics, P.O. Box 85608, San Diego, CA, 92186-5608, USA
2) ITER Organization, Route de Vinon sur Verdon, F-13115 St Paul Lez Durance, France
3) FOM Institute for Plasma Physics Rijnhuizen, Association EURATOM-FOM, 3430 BE
   Nieuwegein, Netherlands
4) Lawrence Livermore National Laboratory, Livermore, CA 94550, USA
5) ASIPP, Hefei, Anhui 230031, China
6) Princeton Plasma Physics Laboratory, PO Box 451, Princeton, NJ 08543, USA
7) University of California-Irvine, Irvine, CA 92697, USA
8) Associação EURATOM/IST, Instituto de Plasmas e Fusão Nuclear, Lisbon, Portugal
9) JAEA, 801-1, Mukouyama, Naka City, Ibaraki, 311-0193, Japan
10) Institute for Plasma Research, Bhat, Gandhinagar, India
11) Columbia University, New York, NY 10027, USA
12) Fusion for Energy Joint Undertaking, Josep Pla. 2, 08019 Barcelona, Spain
13) Association EURATOM-Tekes, Aalto University, FI-00076, AALTO, Finland
14) Oak Ridge National Laboratory, PO Box 2008, Oak Ridge, TN 37831, USA
15) Association EURATOM-Tekes,VTT, FI-02044 VTT, Finland
16) University of California-San Diego, San Diego, CA 92093-0417, USA
17) University of California-Los Angeles, Los Angeles, CA 90095, USA
18) Max Planck Institut für Plasmaphysik, Assoc. EURATOM-MPI, Greifswald, Germany
19) National Fusion Research Institute, Daejeon 305-333, Korea
20) Institute of Tokamak Physics, Russian Research Centre Kurchatov Institute, Moscow, RF
21) FZ Jülich, IEF4-Plasma Physics, Association EURATOM-FZJ, 52428 Jülich, Germany

e-mail contact of main author: schaffer@fusion.gat.com

Abstract. Experiments at DIII-D investigated the effects of ferromagnetic error fields similar to those expected from proposed ITER Test Blanket Modules (TBMs). Studied were effects on: plasma rotation and locking; confinement; L-H transition; edge localized mode (ELM) suppression by resonant magnetic perturbations; ELMs and the H-mode pedestal; energetic particle losses; and more. The experiments used a 3-coil mock-up of 2 magnetized ITER TBMs in one ITER equatorial port. The experiments did not reveal any effect likely to preclude ITER operations with a TBM-like error field. The largest effect was slowed plasma toroidal rotation v across the entire radial profile by as much as $\Delta v/v_0 \sim 50\%$ via non-resonant braking. Changes to global $\Delta n/n$, $\Delta\beta/\beta$ and $\Delta H98/H98$ were ~ 3 times smaller. These effects are stronger at higher β and lower v. Other effects were smaller. The TBM field increased sensitivity to locking by an applied $n=1$ test field, but it was nulled in an L-mode plasma by re-adjusting the DIII-D $n=1$ error field compensation system. Numerical modeling by IPEC reproduces the locking semi-quantitatively and predicts similar compensation of locking in H-mode.

1. Introduction

The proposed ITER tritium-breeding Test Blanket Modules (TBMs) are each expected to contain ~1 tonne of high-temperature and neutron tolerant ferromagnetic steel. Serious deleterious effects were feared based on past experience with toroidal field (TF) ripple from discrete TF coils on tokamak plasmas [1,2]. TF coil and TBM perturbations are both almost entirely non-resonant with the safety factor q of the tokamak axisymmetric field. However, TF coil ripple is periodic while the TBM field would comprise a few localized magnetic "bumps" that generate hundreds of mostly non-resonant helical Fourier harmonics. The effects of TBM perturbations cannot be predicted from present theory. Therefore, a TBM error field mock-up was designed and temporarily installed in an equatorial port at DIII-D to address TBM effects experimentally. An international team and other scientists contributed to planning the experiments, and most of them traveled to the DIII-D site to participate in these experiments in 2009 November. First results were recently presented [3].

2. TBM Error Mock-up and DIII-D Conditions

One large DIII-D equatorial port was temporarily made available to mock up the magnetization of two ITER TBMs installed in one ITER equatorial port. For experimental flexibility the mock-up used copper coils instead of ferromagnetic steel. The magnetization M_T of the steel of two ITER TBMs in the ITER toroidal magnetic field was simulated by two "race track" shaped main coils, visible in Fig. 1. The mockup also had a vertical solenoid to approximate the poloidally directed magnetization M_P of two ITER TBMs. M_P was included to correctly reproduce the very low q-resonant harmonic content of the TBM error field — a general property of the perturbation field of any soft or saturated ferromagnetic object near a tokamak plasma. The distance between the plasma and the mock-up assembly was adjusted by moving the major radius position of either the plasma or the mock-up over a range equivalent to 1 m in ITER. The coil assembly was 0.45 m tall by 0.31 m toroidally by 0.16 m toroidally. We characterize the magnitude of the non axisymmetric perturbing field by a single *local ripple*, $\delta = (B_{max} - B_{min})/(B_{max} + B_{min})$, where B_{max} and B_{min} are the maximum and minimum values of the total toroidal magnetic field B_{tor} at the plasma separatrix in front of the TBM due to the *combined* TBM and toroidal field coil non-axisymmetries. The combined local ripple may be a better plasma physics interaction parameter than the TBM ripple alone. In ITER the TBM plus corrected TF coil local ripple is expected to be $\delta \sim 1.2\%$. The DIII-D mock-up was designed to reach $\delta > 3\%$.

FIG. 1. Drawing of TBM mock-up, showing the two racetrack coils and the vertical solenoid coil. Coils and electrical feeds are red (on line). The coil frame rolls radially on small wheels and can be secured firmly in 12 distinct positions within the re-entrant port. Graphite protective tiles cover the plasma-facing side.

Most experiments were executed in lower-single-null diverted, pumped plasmas with an approximately ITER-similar cross sectional shape, $3.1 \leq q_{95} \leq 4.3$ and normalized beta $(\beta_N) < 2.5$, but occasionally at

higher q_{95} or β_N. The plasma separatrix outer midplane major radius was usually $R_{midout} \approx$ 2.30 m. At this radius the DIII-D toroidal field coil periodic ripple is about 0.35% from 24 coil bundles, which is approximately the same as the ITER target of 0.35%–0.4% periodic ripple from 16 coils after ripple correction. Thus, the DIII-D experiments matched and varied most of the important ITER TBM magnetic field features. Some features could not be matched. First, ITER plans to install 6 TBMs in 3 ports separated by 40° toroidally. This difference introduces an additional extrapolation uncertainty, e.g., which of δ=3% or 2% or 1% in front of one DIII-D port would be the best model of δ=1% in front of 3 ITER ports. Second, because the DIII-D port was proportionately narrower toroidally than an ITER port, the mock-up near field is also narrower. Third, the mock-up coils do not respond to changing plasma fields the same way as ferromagnetic material, but this effect will be small for the strongly saturated steel in ITER TBMs [4].

3. Results of TBM Mock-up Error Field

In this section the results of the TBM mock-up experiments are briefly summarized and discussed by experimental topic.

3.1. Effects on Plasma Rotation

Reduction of the plasma toroidal rotation, $v_T = \Omega R$, was the largest observed effect of the TBM mock-up perturbation. Stable relative velocity reductions $-\Delta v_T/v_{T0}$ up to ~60% were observed at the highest local ripples (~4%) in ELMing H-mode plasmas for the maximum available neutral beam injected (NBI) torque/power ratio. Here $v_{T0} = \Omega_0 R$ is the steady toroidal velocity before application of the perturbation. In H-mode, the relative reductions $-\Delta v_T/v_{T0}$

FIG. 2. Toroidal rotation of C^{6+} measured by charge exchange recombination spectroscopy. Inset shows radial profiles without and with the TBM mock-up field (δ≈3.3%). Main box shows TBM-slowed v_T at $R \approx 2.12$ m as pre-TBM velocity v_{T0} was changed by varying NBI torque shot-by-shot. The mock-up field decreased rotation by an almost constant fraction of pre-TBM Ω across the profile and independently of the injected torque. These are beam-heated ELMing H-mode plasmas. $\beta_N \approx 1.5$, and $R \approx 2.12$ m lies between q=3/2 and q=2.

were roughly 3 times greater than the corresponding relative reductions of density n_e, normalized beta β_N and normalized energy confinement H_{98} (Sec. 3.3). Although the TBM vacuum magnetic field strength decays rapidly into the plasma, the observed relative reductions $-\Delta\Omega/\Omega_0$ extended all the way to the magnetic axis (Fig. 2 inset). The ratio $-\Delta\Omega/\Omega_0$ was approximately uniform across the plasma radius, except near the plasma edge, which had more varied behavior. The absence of local braking at integer-q magnetic surfaces means there is no strong resonant magnetic braking, a conclusion that is consistent with the smallness of the numerically computed $n=1$ harmonic content of the TBM perturbation. Furthermore, $\Delta\Omega \approx -f\Omega_0$ appears to hold well when the NBI torque is varied among similar plasmas with the same local ripple applied (Fig. 2, main box). Here f is a factor independent of torque but dependent on the local ripple and β. Linear dependence of $\Delta\Omega$ on the initial rotation rate is a characteristic of non-resonant neoclassical toroidal viscosity (NTV) braking. NTV braking has been identified in previous experiments in NSTX [5] and DIII-D [6].

Theoretical NTV braking by the mock-up field was evaluated numerically for experimental plasma 140033, using the code IPEC [7] to compute the in-plasma magnetic field, which was then used to calculate the NTV braking torque [Ref. 8 and references therein]. The computed global NTV torque was ~3 times larger than the braking torque inferred from the experiment, good agreement for a calculation that omits dissipation and makes several simplifying approximations. The computed NTV drag peaked at the magnetic axis, which is qualitatively consistent with the observed deep-core braking. The codes identified plasma amplification of the $m,n = 1,1$ ideal internal kink mode, which peaks on axis, as the main cause of the deep-core braking. The computed amplification depends on $q(0)$, the q-profile and β.

3.2. Plasma Rotation Locking

TBM-induced rotation locking was studied in dedicated L- and H-mode plasmas. In both modes the mock-up field decreased plasma tolerance to locking induced by a controlled known $n = 1$ test "error proxy" field.

The Ohmic L-mode plasmas used for locking experiments [9] had a critical line average electron density for locking, $\bar{n}_{\text{crit}}$, of $\approx 0.43 \times 10^{19}$ m^{-3} (Fig. 3, squares at zero current) for the DIII-D intrinsic machine error in 2009 with standard empirical error correction applied. A local TBM ripple of 2.5% approximately doubled the $\bar{n}_{\text{crit}}$ needed for locked mode avoidance (Fig. 3, square at 0.89 kA). This is about the same $\bar{n}_{\text{crit}}$ as for the uncorrected intrinsic error (Fig. 3, diamond). Further Ohmic experiments showed that it was necessary only to re-optimize the standard I-coil $n = 1$ compensation of DIII-D field errors to recover about the same locked mode tolerance as without the mock-up field (Fig. 3, circle). Both the locking threshold increase by the mock-up field and its compensation by the I-coil were matched semi-quantitatively by IPEC calculations,

FIG. 3. Critical locking density $\bar{n}_{\text{crit}}$ in Ohmic L-mode experiments vs. mock-up main coil current. The diamond marks $\bar{n}_{\text{crit}}$ for uncorrected DIII-D intrinsic error field alone. Standard correction of the intrinsic errors was active for data marked by squares. The circle marks $\bar{n}_{\text{crit}}$ after re-optimizing the error correction in the presence of the mock-up field. Local ripple $\delta = 2.5\%$ at 0.9 kA mock-up current.

which demonstrates the strong role of the coupling of error fields to the dominant stable $n = 1$ ideal kink mode [8], even for the spatially localized error field (TBM) that has ~10^2 times more $n > 1$ than $n = 1$ harmonic energy.

ELMing H-mode plasmas could be locked by a high TBM mock-up field at sufficiently unfavorable combinations of high β_N, low q, and low rotation. Figure 4 shows braking and locking in shot 140149 with $\beta_N \approx 2.5$, $q_{95} \approx 3.5$. At $t = 4000$ ms the mock-up current pulse has just reached its steady programmed value for a local ripple $\approx 3.0\%$. Rotation decreased at a

moderate rate across the full profile for the first ~150 ms or so, then the decay rate slowed. At t = 4300 ms rotation was about $0.5 \, \Omega_0$ across most of the profile, but at these higher β_N and δ it never reached a stable steady state. Still, throughout this time there is no sign of stronger braking at any rational surface, e.g. q=1, 3/2 or 2 at $\rho\approx0.4$, 0.6 or 0.7, respectively. This appears like non-resonant braking [6]. Then, starting at about t = 4485 ms, rotation decayed more rapidly, as in classical resonantly braked locking, and by t = 4585 ms the plasma was in a steady locked state. In this final state the locking appears to be strongest near $q\approx1$ and $q\approx3/2$. The q=2 surface at $\rho\approx0.7$ does not seem to be obviously involved in the locking. The TBM field also reduced H-mode plasma tolerance to locking by the

FIG. 4. Evolution of plasma rotation profiles in time from the start of TBM mock-up current flattop. Braking is slow for the first ~450 ms, but is faster by 4485 ms. Runaway braking then leads to a fully locked plasma by t = 4585 ms. $\beta_N \approx 2.5$, the highest used in these experiments, increased braking.

n = 1 test field. Controlled experiments with the test field showed that the initiator of locking was loss of plasma rotation, and that the role of beam torque was only as a means to drive rotation.

IPEC numerical analysis of the H-mode plasma 140033 (β_N=1.5, shown in Fig. 2 inset), revealed plasma amplification of the m,n = 1,1 internal ideal kink mode, which applies NTV braking torque to the inner third of the plasma, despite the edge localized nature of the TBM field. Additional IPEC analysis predicts that a readjusted I-coil n = 1 error correction field should reduce n = 1 NTV braking to a low value and perhaps counteract H-mode locking, as it did in the L-mode locking experiment.

3.3. H-mode Confinement

The TBM mock-up field reduced confinement in H-mode plasmas. The relative reductions depended approximately linearly on local ripple when ripple was varied by changing the mock-up coil current for constant plasma conditions. The local ripple was varied over a range from about 1 to 3 times the expected ITER local ripple in front of TBM ports. Figure 5 shows data from such a scan. The figure also shows that the H-mode global confinement factor H_{98} was affected only about 1/3 as much as the toroidal velocity, v_T.
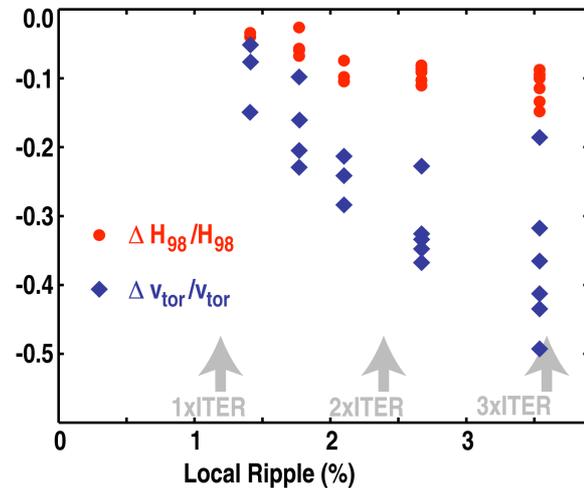
FIG. 5. Relative changes of v_T and H_{98} as a function of local ripple in DIII-D as the mock-up coil current was varied. Other plasma parameters remained constant: R_{midout} = 2.32 m, $q_{95} \approx 3.5$, B_T = 1.7 T, I_p = 1.4 MA, β_N = 2.1~2.4. The local ripple expected in front of ITER TBM ports, ~1.2%, is indicated. The mock-up data extend to about 3 times the expected ITER local ripple.

Figure 6(a) shows that the relative responses of β_N, $\bar{n}_e$ and stored plasma energy W to the mock-up field differed little from H_{98} in Fig. 5. Since neither ion nor electron temperatures were much affected by the mock-up, the changes of β_N, W and H_{98} appear to arise mainly from the decreased $\bar{n}_e$. The responses of $\bar{n}_e$, β_N, W, H_{98} and v_T to the TBM field, including the proportionality factor ~1/3, are quite similar to the confinement degradations and reduced toroidal velocity documented in ITER hybrid scenario plasmas in DIII-D [10], suggesting that all these confinement reductions may be closely linked to v_T or perhaps even caused by it. When the distance between the mock-up and the plasma was increased, the confinement losses decreased less rapidly than linearly with the corresponding local ripple change. Perhaps this weaker dependence is due to the increasing spatial width of the TBM field at the plasma as the two are separated, i.e., because the perturbation field geometry changed.

The magnitudes of the $\bar{n}_e$, W and β_N relative reduction responses to the mock-up field increased with increasing β, especially above $\beta_N=2$ [Fig. 6(b)]. It was difficult to achieve $\beta_N>2.5$ with the ITER-similar shaped ELMing plasmas, and confinement degradation was not studied systematically below $\beta_N\approx1.4$, because it was so small. Plasma rotation was also important, but there were no experiments designed to determine if the rotation reduction was the cause or consequence of other reductions. No obvious dependence of any of these relative responses on collisionality was observed.
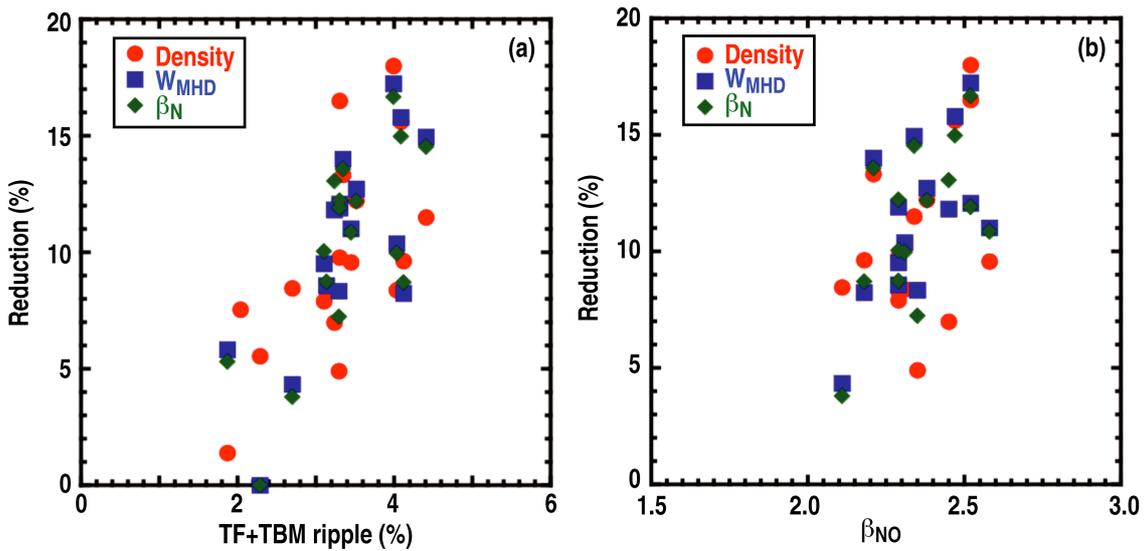
FIG. 6. *Relative responses of* $-\Delta\bar{n}_e/\bar{n}_{e0}$, $-\Delta W/W_0$ *and* $-\Delta\beta_N/\beta_{N0}$ *as a function of (a) local ripple, and (b)* β_{N0}. *These data are selected from shots with* $R_{midout} = 2.30$ m, $q_{95} \sim 3.5$, $B_T = 1.7$ T *and* $I_p = 1.4$ MA. *Data in (a) also satisfy* $\beta_N = 2.1 \sim 2.4$. *Data in (b) satisfy* $\delta > 2.5\%$.

3.4. Small and Null TBM Effects

A local ripple of 2.7% had no measurable effect on either plasma initiation or on locking during the plasma current rise, during an otherwise conventional DIII-D plasma startup, at $B_T = 2.0$ T. The L-H power threshold was unaffected within experimental error by the mock-up field (tested up to $\delta=3.1\%$ at $B_T = 1.7$ T, for co-current and balanced NB and electron cyclotron heating). L-mode plasma confinement was only weakly affected by the mock-up. This is consistent with the weakening of TBM effects with decreasing β.

The TBM mock-up field had no significant effect on ELM characteristics, except that a reduction of Type I ELM frequency was seen in a plasma that was close to an H- to L-mode back transition. The mock-up had no significant effect on the ability of an n=3 resonant magnetic perturbation (RMP) applied by the DIII-D I-coils to suppress Type I ELMs [11].

In the H-mode pedestal, the mock-up appreciably changed only the density, which also changed globally. This rigidity of all the primary pedestal profiles except density is reminiscent of the response of the pedestal plasma to n=3 RMPs applied for ELM suppression [11].

Detailed measurements indicated that global loss of injected neutral beam fast ions due to the TBM mock-up field was small, no greater than the measurement error bars. This experimental result is consistent with calculations by Monte-Carlo fast ion codes [12]. Local heating of the plasma-facing tiles protecting the mock-up was observed, especially when the plasma-tile separation was reduced to ~4 cm. Although the local power loss was too small to be of global significance, ongoing numerical analysis suggests that the enhanced tile heat load could be due at least in part to prompt beam ion losses [13].

The presence or absence of the poloidal magnetization mock-up in addition to the larger toroidal magnetization mock-up had small, barely observable modified effects on confinement.

There are a few examples where the TBM mock-up field appears to enhance the amplitude of MHD activity in the plasma. No consistent effect could be isolated, because most of the experimental H-mode plasmas had irreproducible, time varying, nonlinearly saturated neoclassical tearing mode (NTM) activity. NTM instabilities in these DIII-D plasmas are sensitive to small changes in the plasma radial profiles that were not well controlled.

4. Discussion and Conclusions

The experiments did not reveal any effect likely to preclude ITER operations with a TBM-like error field. The local ripple δ in the DIII-D mock-up experiments was as large as ~3 times the local δ expected in ITER, as one way to compensate for the fact that 3 TBM ports are planned for ITER, but only 1 port was available at DIII-D. This *maximum* mock-up field reduced H-mode energy and confinement by almost 20% at high normalized beta, β_N>2, which is enough to raise concern for the high power-gain ITER mission. The reduction was much smaller for β_N≤1.5. Scaling from DIII-D to ITER is uncertain. The TBM mock-up field exerted significant *non*-resonant braking on plasma toroidal rotation across the whole radial cross section. The mock-up field decreased the plasma tolerance to a known applied test "error" field, but empirical compensation back to the no-TBM tolerance level using the DIII-D error compensation system was demonstrated for a low-β L-mode test plasma. Numerical calculations with IPEC agree semi quantitatively with the experimental rotation braking and plasma locking. The code identifies plasma amplification of the $m,n = 1,1$ ideal internal kink mode, which peaks on axis, as the main cause of the deep-core braking. IPEC also predicts that compensation of locking in high-β H-mode plasmas should be possible wth the DIII-D error compensation system. This would be an important future experiment. TBM field effects on RMP ELM suppression, L-H transition, global fast ion loss and pedestal

properties, (except for pedestal density) were smaller. The theoretical bases to scale these results from DIII-D to ITER are not yet fully clear.

References

[1]   URANO, H., *et al.*, Nucl. Fusion **47** (2007) 706
[2]   DEVRIES, P.C., *et al.*, Nucl. Fusion **48** (2008) 035007
[3]   SNIPES, J.A., *et al.*, Proc. 37th EPS Conf. on Plasma Physics, Dublin (2010) P1.1093
[4]   PUSTOVITOV, V.D., Phys. Plasmas **16** (2009) 052503
[5]   ZHU, W., *et al.*, Phys. Rev. Lett. **49** (2006) 225002
[6]   REIMERDES, H., *et al.*, Nucl. Fusion **49** (2009) 115001
[7]   PARK, J.K., BOOZER, A.H. and GLASSER, A.H., Phys Plasmas **14** (2007) 052110
[8]   PARK, J.K., *et al.*, Phys Plasmas **16** (2009) 056115
[9]   SCOVILLE, J.T. and LA HAYE, R.J., Nucl. Fusion **43** (2003) 250
[10]   POLITZER, P.A., *et al.*, Nucl. Fusion **48** (2008) 075001
[11]   EVANS, T.E., *et al.*, Nucl. Fusion **48** (2008) 024002
[12]   SHINOHARA, K., *et al.*, Fusion Eng. & Design **84** (2009) 24
[13]   KRAMER, G. *et al.*, this conference, EXW/P7-1.